CDF/PUB/BOTTOM/PUBLIC/8523

First Observation of Heavy Baryons Σ_b and Σ_b^*

Text for the blessed web page – CDF note 8523

The CDF Collaboration
URL http://www-cdf.fnal.gov
(Dated: June 28, 2007)

We report an observation of new bottom baryons produced in $p\bar{p}$ collisions at $\sqrt{s} = 1.96$ TeV. Using the fully reconstructed decay mode $\Lambda_b^0 \to \Lambda_c^+ \pi^-$, with $\Lambda_c^+ \to pK^-\pi^+$, we observe the four lowest lying $\Lambda_b^0 \pi^\pm$ resonant states. We interpret these states as the $\Sigma_b^{(*)\pm}$ baryons and measure their masses to be:

$$m_{\Sigma_b^+} = 5807.8^{+2.0}_{-2.2}\ (\text{stat.}) \pm 1.7\ (\text{syst.})\ \text{MeV/c}^2$$
$$m_{\Sigma_b^-} = 5815.2 \pm 1.0\ (\text{stat.}) \pm 1.7\ (\text{syst.})\ \text{MeV/c}^2$$
$$m_{\Sigma_b^{*+}} = 5829.0^{+1.6}_{-1.8}\ (\text{stat.})^{+1.7}_{-1.8}\ (\text{syst.})\ \text{MeV/c}^2$$
$$m_{\Sigma_b^{*-}} = 5836.4 \pm 2.0\ (\text{stat.})^{+1.8}_{-1.7}\ (\text{syst.})\ \text{MeV/c}^2$$

The analysis is based upon 1070 ± 60 pb^{-1} of data collected up to February 2006.

I. INTRODUCTION

Hadron colliders and e^+e^- machines provide a wealth of experimental data on bottom mesons. Yet until recently only one bottom baryon, the Λ_b^0, had been directly observed. Currently the CDF collaboration posseses the world's largest sample of bottom baryons, due to a combination of two factors – the CDF displaced track trigger, and the over 1 fb^{-1} of integrated luminosity delivered by the Tevatron. Using a sample of fully reconstructed $\Lambda_b^0 \to \Lambda_c^+\pi^-$ collected on the displaced track trigger, we search for the decay $\Sigma_b^{(*)\pm} \to \Lambda_b^0\pi^\pm$.

The QCD treatment of quark-quark interactions significantly simplifies if one of the participating quarks is much heavier than the QCD confinement scale $\Lambda_{QCD} \approx 400$ MeV/c^2. In the limit of $m_Q \to \infty$, where m_Q is the mass of the heavy quark, the angular momentum and flavor of the light quark become good quantum numbers. This approach, known as heavy quark effective theory (HQET), thus views a baryon made of one heavy quark and two light quarks as consisting of a heavy static color field surrounded by a cloud corresponding to the light diquark system. In SU(3) the two quarks are in diquark form $\bar{3}$ and 6 according to the decomposition $3 \otimes 3 = \bar{3} \oplus 6$, leading to a generic scheme of baryon classification. Diquark states containing quarks in an antisymmetric flavor configuration, $[q_1, q_2]$, are called Λ-type whereas the states with diquarks containing quarks in a flavor symmetric state, $\{q_1, q_2\}$, are called Σ-type.

In the ground Σ-type state the light diquark has isospin $I = 1$ and $J_l^P = 1^+$. Together with the heavy quark this leads to a doublet of baryons with $J^P = \frac{1}{2}^+$ (Σ_b) and $J^P = \frac{3}{2}^+$ (Σ_b^*). The ground state Σ-type baryons decay strongly to Λ-type baryons by emitting pions. In the limit $m_Q \to \infty$, the spin doublet $\{\Sigma_b, \Sigma_b^*\}$ would be exactly degenerate since an infinitely heavy quark does not have a spin interaction with a light diquark system. As the b quark is not infinitely massive, there will be a mass splitting between the doublet states. There is an additional mass splitting between the $\Sigma_b^{(*)-}$ and $\Sigma_b^{(*)+}$ states due to isospin violation and Coulomb effects.

There exists a variety of predictions for the $\Sigma_b^{(*)}$ masses from non-relativistic and relativistic potential quark models [1–8], $1/N_c$ expansion [9, 10], quark models in the HQET approximation [11–13], sum rules [14, 15], and lattice quantum chromodynamics calculations [16, 17]. A summary of these predictions is presented in Tab. I. The difference between the isospin mass splittings of the Σ_b^* and Σ_b multiplets is predicted to be $[m(\Sigma_b^{*+}) - m(\Sigma_b^{*-})] - [m(\Sigma_b^+) - m(\Sigma_b^-)] = 0.40 \pm 0.07$ MeV/c^2 [18].

Σ_b property	Expected value (MeV/c^2)
m(Σ_b) - m(Λ_b^0)	180 - 210
m(Σ_b^*) - m(Σ_b)	10 - 40
m(Σ_b^-) - m(Σ_b^+)	5 - 7
$\Gamma(\Sigma_b)$, $\Gamma(\Sigma_b^*)$	$\sim$8, $\sim$15

TABLE I: Summary of theoretical expectations for the $\Sigma_b^{(*)\pm}$ states. Predictions are given in Refs. [1] through [17].

The natural width of the Σ_b baryons is expected to be dominated by single pion transitions. Decays of the type $\Sigma_{c,b} \to \Lambda_{c,b}\gamma$ are expected to have significantly smaller (~ 100 keV/c^2) partial widths than the single pion transition, and are thus negligible. The partial width of the P-wave one-pion transition depends on the available phase space. For charmed baryons, this partial width is given by the following equation derived from HQET [19]:

$$\Gamma_{\Sigma_q \to \Lambda_q \pi} = \frac{1}{6\pi} \frac{M_{\Lambda_q}}{M_{\Sigma_q}} |f_p|^2 |\vec{p}_\pi|^3 \quad (1)$$

where q denotes the heavy quark (c or b), and $f_p \equiv g_A/f_\pi$; $g_A = 0.75 \pm 0.05$ is the constituent pion-quark coupling, and $f_\pi = 92$ MeV is the pion decay constant. The momentum of the pion in the Σ_q center of mass frame is $\vec{p}_\pi$. When Eq. (1) is employed for Σ_c and Λ_c^+ (*i.e.*, $q \equiv c$), it predicts widths for the $\Sigma_c^{(*)}$ baryons which are in excellent agreement with the PDG data [20]. For the range of predicted $\Sigma_b^{(*)}$ masses, Eq. (1) predicts natural widths $\Gamma(\Sigma_b^{(*)})$ between 2 and 20 MeV/c^2.

II. ANALYSIS STRATEGY

The present analysis is based on events collected by the CDF II detector from February 2002 through February 2006, with an integrated luminosity of $\mathcal{L} = 1070 \pm 60$ pb^{-1}. Events collected on the two displaced track trigger are used to reconstruct the decay chain $\Lambda_b^0 \to \Lambda_c^+\pi$, with $\Lambda_c^+ \to pK^-\pi^+$. The selection criteria for Λ_b^0 reconstruction are listed in Tab. II. The fit to the invariant $\Lambda_c^+\pi^-$ mass distribution, shown in Fig. 1, results in 3180 ± 60 (stat.) $\Lambda_b^0 \to \Lambda_c^+\pi^-$ candidates.

Variable	Cut value
	B_CHARM_SCENA
$p_T(\pi_b^-)$	> 2 GeV/c
$p_T(p)$	> 2 GeV/c
$p_T(p)$	$> p_T(\pi^+)$
$p_T(K^-)$	> 0.5 GeV/c
$p_T(\pi^+)$	> 0.5 GeV/c
$ct(\Lambda_b^0)$	> 250 μm
$ct(\Lambda_b^0)/\sigma_{ct}$	> 10
$\lvert d_0(\Lambda_b^0)\rvert$	< 80 μm
$ct(\Lambda_c^+ \leftarrow \Lambda_b^0)$	> -70 μm
$ct(\Lambda_c^+ \leftarrow \Lambda_b^0)$	< 200 μm
$\lvert m(pK^-\pi^+) - m(\Lambda_c^+)_{PDG}\rvert$	< 16 MeV/c^2
$p_T(\Lambda_b^0)$	> 6.0 GeV/c
$p_T(\Lambda_c^+)$	> 4.5 GeV/c
Prob(χ^2_{3D}) of Λ_b^0 vertex fit	$> 0.1\%$

TABLE II: Analysis cuts determined for Λ_b reconstruction.

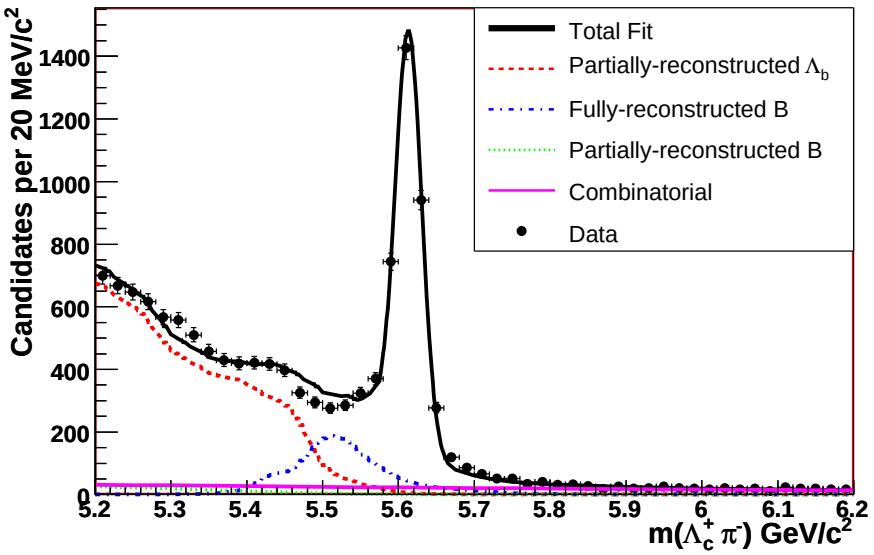

FIG. 1: Fit to the invariant mass of $\Lambda_b^0 \to \Lambda_c^+\pi^-$ candidates. Fully reconstructed Λ_b^0 decays such as $\Lambda_b^0 \to \Lambda_c^+\pi^-$ and $\Lambda_b^0 \to \Lambda_c^+K^-$ are not indicated on the figure. The Λ_b^0 signal region, $m(\Lambda_c^+\pi^-) \in [5.565, 5.670]$ GeV/c^2, consists primarily of Λ_b^0 baryons, with some contamination from B mesons and combinatorial events. The discrepancies between the fit and data below the Λ_b^0 signal region are due to incomplete knowledge of the branching ratios of the decays in this region and are included in the $\Sigma_b^{(*)}$ sample composition systematic uncertainties.

To separate out the resolution on the mass of each Λ_b^0 candidate, we search for narrow Σ_b resonances in the mass difference distribution of $Q = m(\Lambda_b^0\pi) - m(\Lambda_b^0) - m_\pi$. Unless explicitly stated, Σ_b refers to both the $J = \frac{1}{2}$ ($\Sigma_b^\pm$) and $J = \frac{3}{2}$ ($\Sigma_b^{*\pm}$) states. The pion from Σ_b decay, denoted π_{Σ_b}, is required to pass all default track quality cuts. There is no transverse momentum (p_T) cut applied since these are expected to be very soft tracks. In order to perform an unbiased search, the cuts for Σ_b reconstruction are optimized with the Σ_b signal region blinded. From theoretical predictions the Σ_b signal region is chosen as $30 < Q < 100$ MeV/c^2; the upper and lower sideband regions of $0 < Q < 30$ MeV/c^2 and $100 < Q < 500$ MeV/c^2 represent the Σ_b background. The signal for the optimization is taken from a Σ_b PYTHIA [21] Monte Carlo sample, with the decays $\Sigma_b \to \Lambda_b^0\pi$, $\Lambda_b^0 \to \Lambda_c^+\pi^-$, and $\Lambda_c^+ \to pK^-\pi^+$ forced. The optimization is performed for the following variables: the p_T of the Σ_b candidate, the impact parameter significance $|d_0/\sigma_{d_0}|$ of the π_{Σ_b} track, and the $\cos\theta^*$ of the π_{Σ_b} track. The angle θ^* is defined between the momentum of π_{Σ_b} in the Σ_b rest frame and the direction of total Σ_b momentum in the lab frame. A simultaneous optimization of all three criteria yields the cut values listed in Tab. III.

Variable	Cut value	Step size
$p_{\rm T}(\Sigma_b)$	> 9.5 GeV/c	0.5 GeV/c
$\lvert d_0/\sigma_{d_0}\rvert\ (\pi_{\Sigma_b})$	< 3.0	0.25
$\cos\theta^*\ (\pi_{\Sigma_b})$	> -0.35	0.05

TABLE III: Selection criteria determined for Σ_b reconstruction and the step sizes used by the optimization algorithm.

After optimization of the selection criteria, Σ_b events are separated into "$\Lambda_b^0\pi^-$" and "$\Lambda_b^0\pi^+$" subsamples. As Λ_b^0 is neutral, the charge of the soft pion track determines the charge of the Σ_b, and there will be Σ_b signal for both positive and negative pions. The $\Lambda_b^0\pi^-$ subsample is defined as events where the Σ_b pion has the same charge as the pion from Λ_b^0, and the $\Lambda_b^0\pi^+$subsample as events where the Σ_b pion charge is the opposite of the Λ_b^0 pion's charge. With these definitions, the $\Lambda_b^0\pi^-$ subsample contains $\Sigma_b^{(*)-}$ and $\overline{\Sigma}_b^{(*)-}$ while the $\Lambda_b^0\pi^+$ subsample contains $\Sigma_b^{(*)+}$ and $\overline{\Sigma}_b^{(*)+}$.

The backgrounds under the Λ_b^0 signal region in the Λ_b^0 mass distribution will also be present in the Σ_b Q distribution. The primary sources of background are:

- Tracks from the hadronization of prompt Λ_b^0 baryons
- Tracks from the hadronization of B mesons reconstructed as Λ_b^0 baryons
- Combinatorial background

The underlying event tracks also contribute, but since they cannot be separated from the hadronization tracks, we use "hadronization" to denote the sum of the two contributions. The percentage of each background component in the Λ_b^0 signal region is derived from the Λ_b^0 mass fit, and is given in Tab. IV. Other backgrounds (*e.g.* from 5-track decays where one track is taken as the π_{Σ_b} candidate) are negligible, as confirmed in inclusive single b hadron Monte Carlo samples [22, 23]. The Q shape and normalization of each background source is fixed before unblinding the Σ_b signal region. The high mass region above the $\Lambda_b^0 \to \Lambda_c^+\pi^-$ signal in Fig. 1 determines the combinatorial background. Reconstructing $\overline{B^0} \to D^+\pi^-$ data as $\Lambda_b^0 \to \Lambda_c^+\pi^-$ gives the B hadronization background. The largest background component, the Λ_b^0 hadronization, is obtained from a generic $\Lambda_b^0 \to \Lambda_c^+\pi^-$ PYTHIA Monte Carlo sample. The Λ_b^0 $p_{\rm T}$ spectrum of the PYTHIA sample is reweighted to agree with the spectrum from data. The PYTHIA sample has fewer soft tracks around the Λ_b^0 than found in data, so the $p_{\rm T}$ spectrum of tracks is also reweighted to agree with data. After reweighting, the shape and normalization of the Λ_b^0 hadronization from PYTHIA agree with the Q sideband distributions, as shown in Fig. 2 (left).

Λ_b^0 Sample Composition $m(\Lambda_b^0) \in [5.565, 5.670]$ GeV/c^2	
Λ_b^0	$(89.5 \pm 1.7)\%$
B	$(7.2 \pm 0.6)\%$
Comb. Bkg.	$(3.3 \pm 0.1)\%$

TABLE IV: Sample composition in the Λ_b^0 signal region.

III. RESULTS

Upon unblinding the Q signal region, there is an excess observed in data over the predicted backgrounds. The excess over background is shown in Fig. 2 (right) and given in Tab. V.

We then perform a simultaneous unbinned maximum likelihood fit to $\Lambda_b^0\pi^-$ and $\Lambda_b^0\pi^+$ subsamples. To the already described background components we add four peaks, one for each of the expected Σ_b states. Each peak consists of a Breit-Wigner distribution convoluted with a double Gaussian detector resolution model. This detector resolution model has a dominant narrow core and a small broader shape describing the tails. The natural width of each Breit-Wigner is computed from Eq. (1), where M_{Σ_q} is set to be the location of the peak. The peaks are thus increasing in breadth from left to right. The expected difference of the isospin mass splittings within the Σ_b^* and Σ_b multiplets is below our sensitivity with this sample of data. Consequently, we constrain $m(\Sigma_b^{*+}) - m(\Sigma_b^+) = m(\Sigma_b^{*-}) - m(\Sigma_b^-)$ and measure an average hyperfine mass splitting $m(\Sigma_b^*) - m(\Sigma_b)$. The four Σ_b signal fit to data, which has a fit probability of 76% in the range $Q \in [0, 200]$ MeV/c^2, is shown in Fig. 3 with the fit results given in Tab. VI.

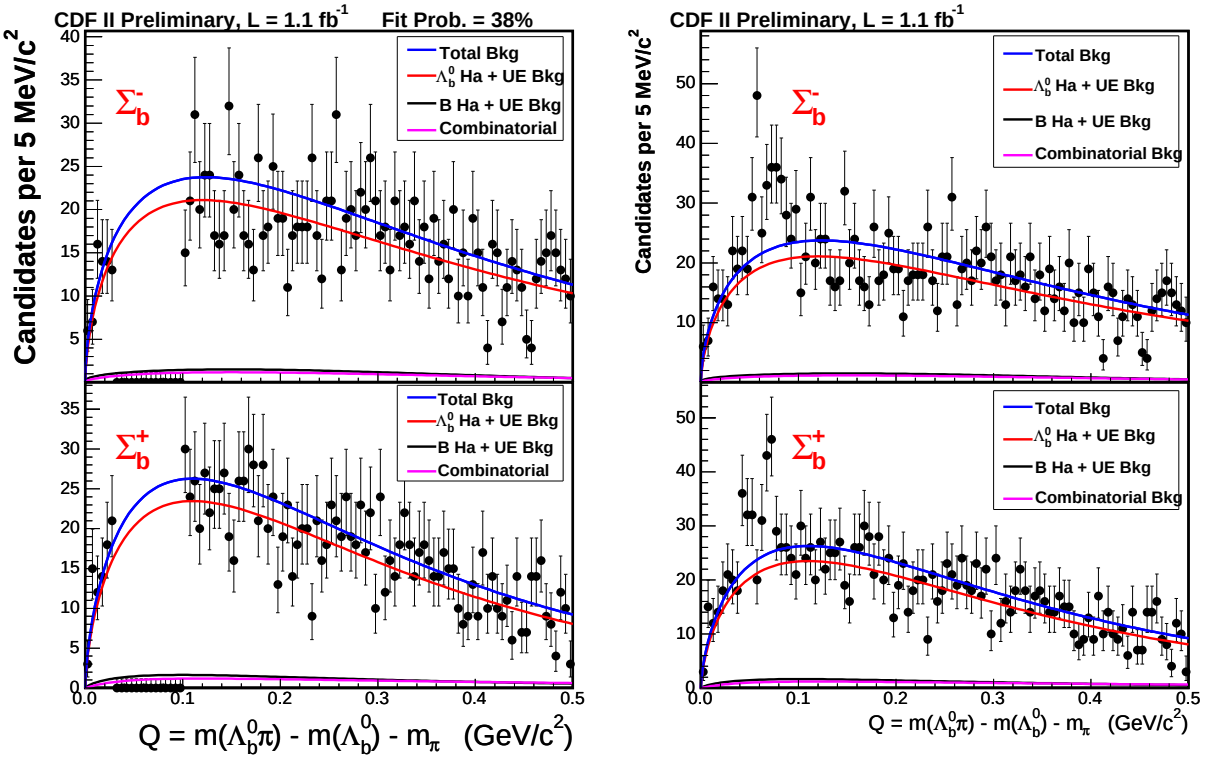

FIG. 2: The three background sources described in Sec. II and their sum are shown superimposed on the Q distributions in data. The $\Lambda_b^0\pi^-$ subsample is shown in the top distribution, while the $\Lambda_b^0\pi^+$ subsample is shown in the bottom distribution. To the left is the plot with the signal region blinded, while on the right is the plot with the signal region unblinded.

Sample	Data events	Bkg events	Data excess over bkg
$\Lambda_b^0\pi^-$	406	288	118
$\Lambda_b^0\pi^+$	404	313	91

TABLE V: Summary of the number of events in the Q signal region ($Q \in [0.03, 0.1]$ GeV/c^2) for the data and the predicted background.

Parameter	Value	Parabolic Error	MINOS Errors
Σ_b^+ Q (MeV/c^2)	48.5	1.97	(+1.98, -2.17)
Σ_b^- Q (MeV/c^2)	55.9	0.951	(+0.973, -0.950)
$\Sigma_b^* - \Sigma_b$ Q (MeV/c^2)	21.2	1.92	(+2.00, -1.94)
Σ_b^+ events	32	12.1	(+12.5, -11.7)
Σ_b^- events	59	14.2	(+14.6, -13.7)
Σ_b^{*+} events	77	16.8	(+17.3, -16.3)
Σ_b^{*-} events	69	17.6	(+18.0, -17.1)
-ln(Likelihood)	-24160.4	–	–

TABLE VI: Fit parameter and error values from the fit to data. Positive and negative errors are quoted separately as the error range is asymmetric.

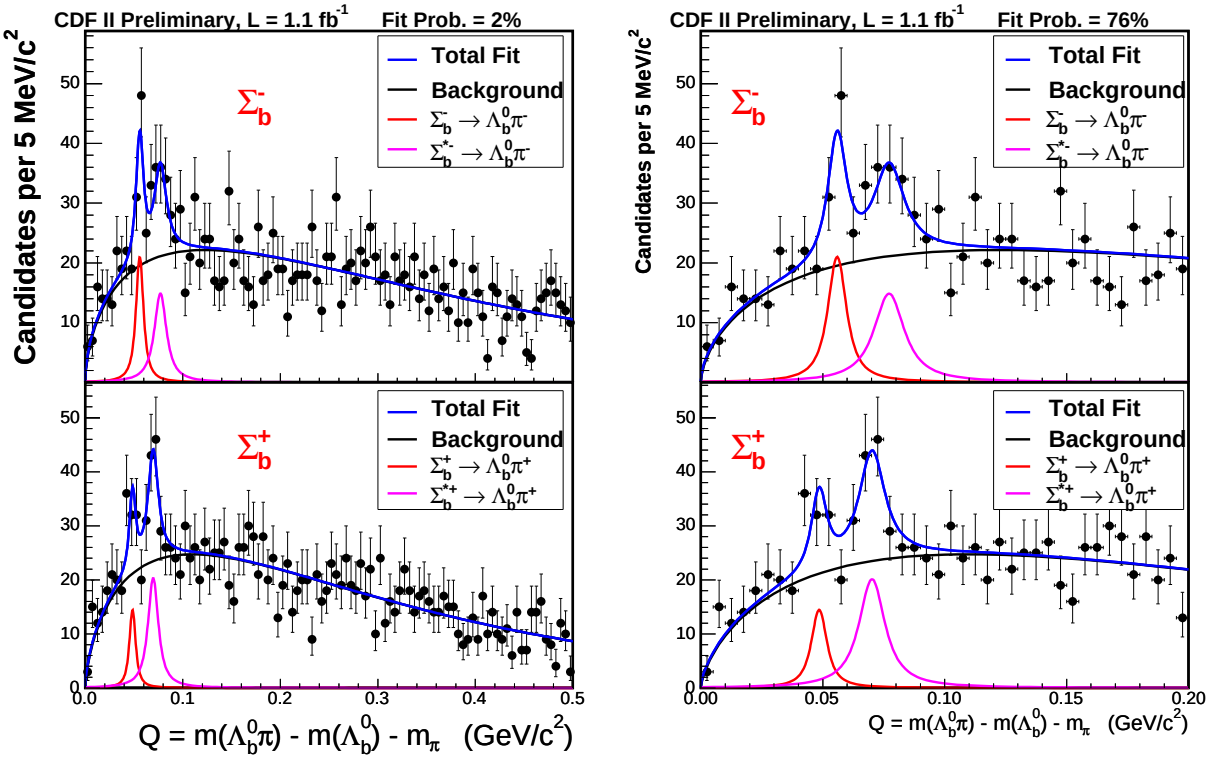

FIG. 3: Simultaneous fit to the $\Lambda_b^0\pi^-$ and $\Lambda_b^0\pi^+$ Σ_b signal. To the left is the full Q range of [0, 500] MeV/c^2 while on the right is a smaller region around the signal peaks ($Q \in$ [0, 200] MeV/c^2).

A. Systematics

All systematic uncertainties on the mass difference measurements are small compared to the statistical uncertainties, and are summarized in Tab. VII. To determine the mass scale uncertainty, we compare the measured masses of the D^*, Σ_c^0, Σ_c^{++}, and Λ_c^* particles with the world average values quoted in the PDG [20]. For these decays which release little kinetic energy, the figure of merit is the Q value. In a previous analysis, it has been shown that the systematic error on this Q value may be approximated as linear, $\delta Q = a \cdot Q + \delta m(Q = 0)$ [24]. We plot the difference between the CDF and PDG mass measurements as a function of the Q value of the decay, and fit the graph to a linear function. This function is evaluated at the Σ_b Q value to estimate the systematic uncertainty. This is the largest systematic uncertainty on the Q measurements, ranging from 0.1 to 0.3 MeV/c^2.

In addition to the mass scale systematic, there are systematic uncertainties which are built into the assumptions of the Σ_b fit. Taking the fit parameters associated with one assumption, we generate simplistic Monte Carlo samples where these parameters are varied. Each sample is fit with both the default fit and the fit with varied parameters. We then take the difference between the parameter values in the varied fit and the default fit. This difference, caused by the systematic variation, constitutes the systematic uncertainty from this assumption. After generating 500 Monte Carlo samples, we model the distribution of this difference with a Gaussian and take the mean of the Gaussian as the systematic shift due to that systematic uncertainty. The fit systematics we consider, also summarized in Tab. VII, are:

- Sample composition of the Λ_b^0 signal region ("Λ_b^0 Comp.")
- Normalization and functional form of the Λ_b^0 hadronization background ("Λ_b^0 Norm." and "Λ_b^0 Shape")
- Change of the Λ_b^0 hadronization background shape due to extreme changes in the track $p_{\rm T}$ spectrum used to reweight the PYTHIA Monte Carlo sample ("Reweight")
- Underestimation of the detector resolution ("Reso.")
- Uncertainty in the Σ_b intrinsic width prediction ("Σ_b Width")
- Constraint $m(\Sigma_b^{*+}) - m(\Sigma_b^+) = m(\Sigma_b^{*-}) - m(\Sigma_b^-)$ ("Δ_*")

Parameter	Mass Scale	Λ_b^0 Comp.	Λ_b^0 Norm.	Λ_b^0 Shape	Reweight	Reso.	Σ_b Width	Δ_*	Total
Σ_b^- Q	0.22	0.0	0.009	0.0	0.04	0.0	0.009	0.06	0.23
	-0.22	-0.03	-0.002	-0.011	-0.0004	-0.011	-0.005	0.0	-0.22
Σ_b^- events	0.0	0.7	2.2	0.3	7.4	0.3	3.4	0.0	8.5
	0.0	0.0	-2.2	0.0	0.0	0.0	-3.4	-0.08	-4.1
Σ_b^+ Q	0.19	0.03	0.013	0.013	0.0	0.0	0.01	0.0	0.19
	-0.19	0.0	-0.013	0.0	-0.11	-0.014	-0.02	-0.11	-0.25
Σ_b^+ events	0.0	3.3	2.1	1.2	2.3	0.3	1.8	0.0	5.0
	0.0	0.0	-2.1	0.0	-1.8	0.0	-2.0	-0.004	-3.4
Σ_b^{*-} events	0.0	0.4	4.8	0.3	14.7	0.1	1.7	0.0	15.6
	0.0	0.0	-4.7	0.0	0.0	0.0	-1.7	-0.16	-5.0
Σ_b^{*+} events	0.0	7.3	4.8	2.8	4.6	0.2	0.8	0.16	10.3
	0.0	0.0	-4.8	0.0	-2.9	0.0	-0.8	0.0	-5.7
$\Sigma_b^* - \Sigma_b$ Q	0.10	0.05	0.14	0.04	0.32	0.02	0.07	0.0	0.38
	-0.10	0.0	-0.13	0.0	0.0	0.0	-0.07	-0.26	-0.32
Σ_b^{*-} Q	0.28	0.02	0.13	0.03	0.32	0.003	0.08	0.0	0.45
	-0.28	0.0	-0.13	0.0	0.0	0.0	-0.07	-0.184	-0.37
Σ_b^{*+} Q	0.32	0.09	0.12	0.05	0.17	0.001	0.05	0.0	0.40
	-0.32	0.0	-0.13	0.0	0.0	0.0	-0.06	-0.39	-0.52

TABLE VII: Systematic uncertainties on the Σ_b measurement. All Q values are in units of MeV/c^2. Because some of the effects are highly asymmetric, positive and negative errors are separately added in quadrature. While we fit for the Σ_b^-, Σ_b^+, and $\Sigma_b^* - \Sigma_b$ Q values, we also separately evaluate the systematic uncertainties on the Σ_b^{*-} and Σ_b^{*+} Q values so that all four masses can be quoted directly.

B. Significance

To evaluate the significance of the measurement, there are three questions to ask:

1. Is the data consistent with the null (*ie* no signal) hypothesis?
2. Is the data consistent with a two peak hypothesis, *i.e.* what is the significance of the dip between the Σ_b and Σ_b^* signals?
3. What is the significance of each individual peak?

To answer these questions, the data is fit with an alternate signal hypothesis: no signal, two Σ_b states (one per $\Lambda_b^0\pi$ charge combination), or three Σ_b states, performed by eliminating one of the states in the four signal hypothesis. We then compute a likelihood ratio:

$$LR = \frac{L_1}{L_2} = \frac{e^{-NLL_1}}{e^{-NLL_2}} = e^{NLL_2 - NLL_1} \tag{2}$$

where L_1 is the likelihood of the four signal peak hypothesis, L_2 is that of the alternate hypothesis, and NLL stands for the negative log likelihood ($-\ln(L)$). Systematic variations are included in the fits as nuisance parameters over which the likelihood is integrated. The results of the no signal and two Σ_b states fits to data are shown in Fig. 4.

After measuring the likelihood ratios in data, we use the LR as a test statistic to determine a p-value. We generate simplistic Monte Carlo samples from one of the alternate hypotheses and fit each sample with both the four signal hypothesis and the alternate hypothesis. We evaluate the likelihood difference between the fits and obtain a probability density $P_{\rm bkg}(NLL_2 - NLL_1)$ to observe at least a likelihood difference of $NLL_2 - NLL_1$ for the four signal fit on an alternate hypothesis sample. We then use the measured likelihood difference in data and integrate $P_{\rm bkg}(NLL_2 - NLL_1)$ from $(NLL_2 - NLL_1)^{\rm data}$ to infinity. That integral divided by the total number of Monte Carlo samples generated is the p-value.

The measured likelihood differences, p-values, and equivalent standard deviations from the normal distribution are given in Tab. VIII. For the background only hypothesis, we generated 12 million Monte Carlo samples and none had a likelihood difference close to that seen in data. Thus, the no signal p-value is only an upper limit, and the background only hypothesis is excluded at greater than the 5 σ level. Each of the four peaks has > 3 σ significance except for the Σ_b^+ peak.

IV. SUMMARY

The lowest lying $\Lambda_b^0\pi^\pm$ resonant states are observed in 1.1 fb^{-1} of data collected by the CDF II detector, and they are consistent with the lowest lying $\Sigma_b^{(*)\pm}$ baryons. The Σ_b^- and Σ_b^+ Q values and the average $\Sigma_b^* - \Sigma_b$ mass splitting are measured to be:

Hypothesis	$(NLL_2 - NLL_1)^{\text{data}}$	p-value	Significance (σ)
No signal	42.4	$< 8.3 \times 10^{-8}$	> 5.23
Two peaks	15.3	9.2×10^{-5}	3.74
No Σ_b^- Peak	11.7	3.2×10^{-4}	3.41
No Σ_b^+ Peak	3.9	9.0×10^{-3}	2.36
No Σ_b^{*-} Peak	10.8	6.4×10^{-4}	3.22
No Σ_b^{*+} Peak	11.3	6.0×10^{-4}	3.24

TABLE VIII: Likelihood ratio p-values for the alternate signal hypotheses, where NLL_2 denotes the negative log likelihood of the alternate hypothesis and NLL_1 that of the four signal hypothesis. For the no signal hypothesis, no events were observed with the significance seen in data, and the p-value is only an upper limit.

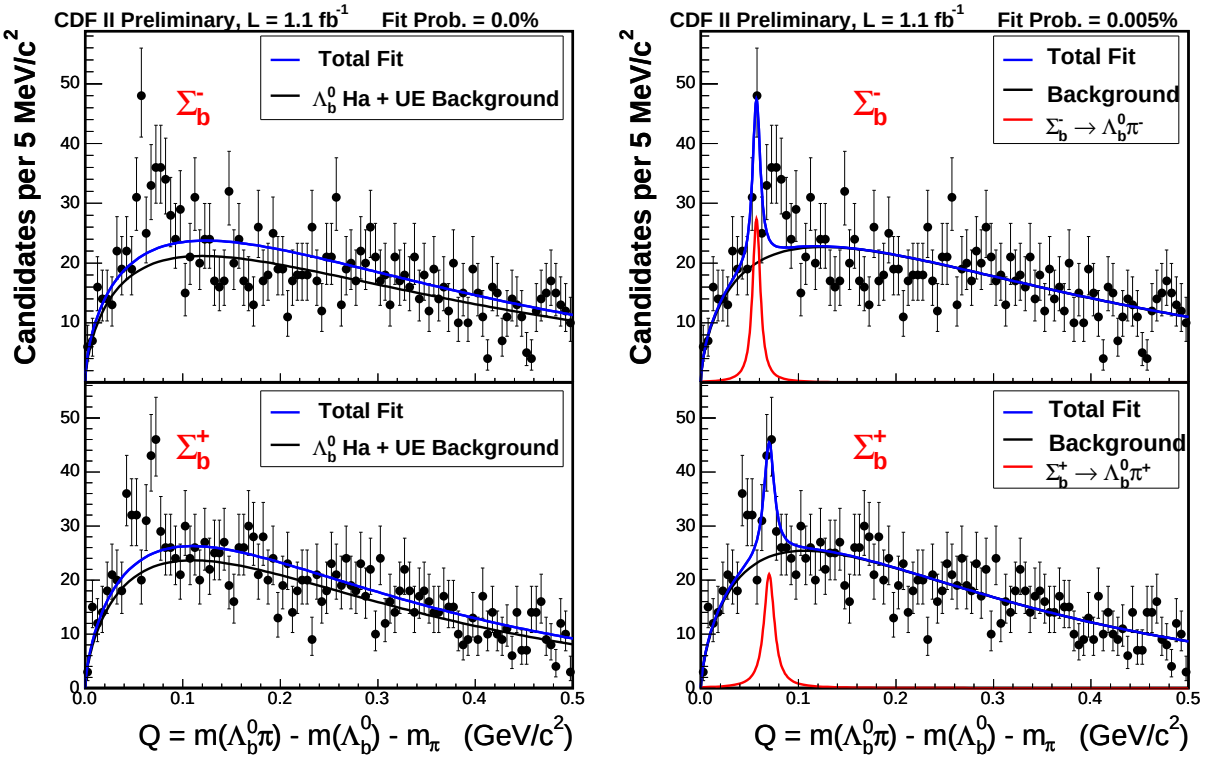

FIG. 4: Fits with alternate signal descriptions. On the left is the null hypothesis assumption, with no signal present. On the right is the two peak assumption, with a fit to one peak in $\Lambda_b^0\pi^-$ and one peak in $\Lambda_b^0\pi^+$.

$$m(\Sigma_b^+) - m(\Lambda_b^0) - m(\pi) = 48.5^{+2.0}_{-2.2}\ (\text{stat.})\ ^{+0.2}_{-0.3}\ (\text{syst.})\ \text{MeV}/c^2$$

$$m(\Sigma_b^-) - m(\Lambda_b^0) - m(\pi) = 55.9 \pm 1.0\ (\text{stat.})\ \pm 0.2\ (\text{syst.})\ \text{MeV}/c^2$$

$$m(\Sigma_b^{*-}) - m(\Sigma_b^-) = m(\Sigma_b^{*+}) - m(\Sigma_b^+) = 21.2^{+2.0}_{-1.9}\ (\text{stat.})\ ^{+0.4}_{-0.3}\ (\text{syst.})\ \text{MeV}/c^2$$

Using the recent CDF II mass measurement of $m(\Lambda_b^0) = 5619.7 \pm 1.2\ (\text{stat.})\ \pm 1.2\ (\text{syst.})\ \text{MeV}/c^2$ [24], the absolute mass values and number of events for each Σ_b state are:

$$m(\Sigma_b^+) = 5807.8^{+2.0}_{-2.2}\ (\text{stat.})\ \pm 1.7\ (\text{syst.})\ \text{MeV}/c^2 \quad \text{N}(\Sigma_b^+) = 32^{+13}_{-12}\ (\text{stat.})\ ^{+5}_{-3}\ (\text{syst.})$$

$$m(\Sigma_b^-) = 5815.2 \pm 1.0\ (\text{stat.})\ \pm 1.7\ (\text{syst.})\ \text{MeV}/c^2 \quad \text{N}(\Sigma_b^-) = 59^{+15}_{-14}\ (\text{stat.})\ ^{+9}_{-4}\ (\text{syst.})$$

$$m(\Sigma_b^{*+}) = 5829.0^{+1.6}_{-1.8}\ (\text{stat.})\ ^{+1.7}_{-1.8}\ (\text{syst.})\ \text{MeV}/c^2 \quad \text{N}(\Sigma_b^{*+}) = 77^{+17}_{-16}\ (\text{stat.})\ ^{+10}_{-6}\ (\text{syst.})$$

$$m(\Sigma_b^{*-}) = 5836.4 \pm 2.0\ (\text{stat.})\ ^{+1.8}_{-1.7}\ (\text{syst.})\ \text{MeV}/c^2 \quad \text{N}(\Sigma_b^{*-}) = 69^{+18}_{-17}\ (\text{stat.})\ ^{+16}_{-5}\ (\text{syst.})$$

Acknowledgments

We thank T. Becher, A. Falk, D. Pirjol, J. Rosner, and D. Ebert for useful discussions. We also thank the Fermilab staff and the technical staffs of the participating institutions for their vital contributions. This work was supported by the U.S. Department of Energy and National Science Foundation; the Italian Istituto Nazionale di Fisica Nucleare; the Ministry of Education, Culture, Sports, Science and Technology of Japan; the Natural Sciences and Engineering Research Council of Canada; the National Science Council of the Republic of China; the Swiss National Science Foundation; the A.P. Sloan Foundation; the Bundesministerium für Bildung und Forschung, Germany; the Korean Science and Engineering Foundation and the Korean Research Foundation; the Particle Physics and Astronomy Research Council and the Royal Society, UK; the Institut National de Physique Nucleaire et Physique des Particules/CNRS; the Russian Foundation for Basic Research; the Comisión Interministerial de Ciencia y Tecnología, Spain; the European Community's Human Potential Programme under contract HPRN-CT-2002-00292; and the Academy of Finland.

[1] D. P. Stanley and D. Robson, Phys. Rev. Lett. **45**, 235 (1980).
[2] D. P. Stanley and D. Robson, Phys. Rev. D **21**, 3180 (1980).
[3] D. Izatt, C. DeTar, and M. Stephenson, Nucl. Phys. **B199**, 269 (1982).
[4] J. M. Richard and P. Taxil, Phys. Lett. B **128**, 453 (1983).
[5] J. L. Basdevant and S. Boukraa, Z. Phys. C **30**, 103 (1986).
[6] W. Y. P. Hwang and D. B. Lichtenberg, Phys. Rev. D **35**, 3526 (1987).
[7] A. Martin and J. M. Richard, Phys. Lett. B **185**, 426 (1987).
[8] D. B. Lichtenberg, R. Roncaglia, J. G. Wills, and E. Predazzi, Z. Phys. C **47**, 83 (1990).
[9] E. Jenkins, Phys. Rev. D **54**, 4515 (1996).
[10] E. Jenkins, Phys. Rev. D **55**, 10 (1997).
[11] C. Albertus, J. E. Amaro, E. Hernandez, and J. Nieves, Nucl. Phys. **A740**, 333 (2004).
[12] D. Ebert, R. N. Faustov, and V. O. Galkin, Phys. Rev. D **72**, 034026 (2005).
[13] S. Capstick, Phys. Rev. D **36**, 2800 (1987).
[14] R. Roncaglia, D. B. Lichtenberg, and E. Predazzi, Phys. Rev. D **52**, 1722 (1995).
[15] M. Karliner and H. J. Lipkin, hep-ph/0307243; condensed version in Phys. Lett. B **575**, 249 (2003).
[16] K. C. Bowler *et al.* (UKQCD Collaboration), Phys. Rev. D **54**, 3619 (1996).
[17] N. Mathur, R. Lewis, and R. M. Woloshyn, Phys. Rev. D **66**, 014502 (2002).
[18] J. L. Rosner, Phys. Rev. D **57**, 4310 (1998). J. L. Rosner, Phys. Rev. D **75**, 013009 (2007).
[19] J. G. Körner, M. Krämer, and D. Pirjol, Prog. Part. Nucl. Phys. **33**, 787 (1994).
[20] W. M. Yao *et al.* (Particle Data Group), J. Phys. G **33**, 1 (2006).
[21] T. Sjöstrand, P. Eden, C. Friberg, L. Lonnblad, G. Miu, S. Mrenna, and E. Norrbin, Comput. Phys. Commun. **135**, 238 (2001).
[22] We use a variety of single b hadron simulations, all using the $p_{\mathrm{T}}(B)$ and $y(B)$ distributions obtained from B decays in data (D. Acosta *et al.* (CDF Collaboration), Phys. Rev. D **71**, 032001 (2005)). The simulated $p_{\mathrm{T}}(\Lambda_b^0)$ distribution is reweighted to match the sideband-subtracted data.
[23] The b hadrons are decayed using the EvtGen package, D. J. Lange, Nucl. Instrum. Methods A **462**, 152 (2001).
[24] D. Acosta *et al.* [CDF Collaboration], Phys. Rev. Lett. **96**, 202001 (2006).